Ultrafast all-optical Nth-order differentiator and simultaneous repetition-rate multiplier of periodic pulse train

Miguel A. Preciado and Miguel A. Muriel

ETSI Telecomunicacion, Universidad Politecnica de Madrid (UPM), 28040 Madrid, Spain.
miguel.preciado@tfo.upm.es, muriel@tfo.upm.es

Abstract: The letter presents a technique for Nth-order differentiation of periodic pulse train, which can simultaneously multiply the input repetition rate. This approach uses a single linearly chirped apodized fiber Bragg grating, which grating profile is designed to map the spectral response of the Nth-order differentiator, and the chirp introduces a dispersion that, besides space-to-frequency mapping, it also causes a temporal Talbot effect.

OCIS codes: (060.2340) Fiber optics components; (230.1150) All-optical devices; (320.5540) Pulse shaping; (999.9999) Fiber Bragg gratings.

References and Links

1. H. J. A. da Silva and J. J. O'Reilly, "Optical pulse modeling with Hermite - Gaussian functions," Opt. Lett. **14**, 526- (1989).
2. R. Slavík, Y. Park, M. Kulishov, R. Morandotti, and J. Azaña, "Ultrafast all-optical differentiators ," Opt. Express **14**, 10699-10707 (2006).
3. N. K. Berger, B. Levit, B. Fischer, M. Kulishov, D. V. Plant, and J. Azaña, "Temporal differentiation of optical signals using a phase-shifted fiber Bragg grating," Opt. Express **15**, 371-381 (2007).
4. M. Kulishov and J. Azaña, "Design of high-order all-optical temporal differentiators based on multiple-phase-shifted fiber Bragg gratings," Opt. Express **15**, 6152-6166 (2007).
5. Y. Park, R. Slavik, J. Azaña "Ultrafast all-optical first and higher-order differentiators based on interferometers" Opt. Lett. **32**, 710-712 (2007).
6. M. A. Preciado, V. García-Muñoz, and M. A. Muriel "Ultrafast all-optical Nth-order differentiator based on chirped fiber Bragg gratings," Opt. Express **15**, 7196-7201 (2007).
7. A. G. Jepsen, A. E. Johnson, E. S. Maniloff, T. W. Mossberg, M. J. Munroe, and J. N. Sweetser, "Fibre Bragg grating based spectral encoder/decoder for lightwave CDMA," Electron. Lett. **35**, 1096-1097 (1999).
8. M. A. Preciado, V. García-Muñoz, and M. A. Muriel "Grating design of oppositely chirped FBGs for pulse shaping," IEEE Photon. Technol. Lett. **19**, 435-437 (2007).
9. J. Azaña and L. R. Chen, "Synthesis of temporal optical waveforms by fiber Bragg gratings: a new approach based on space-to-frequency-to-time mapping ," J. Opt. Soc. Am. B **19**, 2758-2769 (2002).
10. S. Longhi, M. Marano, P. Laporta, and V. Pruneri, "Multiplication and reshaping of high-repetition-rate optical pulse trains using highly dispersive fiber Bragg gratings," IEEE Photon. Technol. Lett. **12**, 1498–1500 (2000).
11. S. Longhi, M. Marano, P. Laporta, O. Svelto, "Propagation, manipulation, and control of picosecond optical pulses at 1.5 μm in fiber Bragg gratings, J. Opt. Soc. Am. B **19**, 2742-2757 (2002).
12. J. Azaña and M. A. Muriel, "Temporal Talbot effect in fiber gratings and its applications," Appl. Opt. **38**, 6700-6704 (1999).
13. J. Azaña and M. A. Muriel, ''Real-time optical spectrum analysis based on the time-space duality in chirped fiber gratings,'' IEEE J. Quantum Electron. **36**, 517–527 (2000).
14. J. T. Mok and B. J. Eggleton, "Impact of group delay ripple on repetition-rate multiplication through Talbot self-imaging effect," Opt. Commun. **232**, 167-178, (2004).

1. Introduction

The letter presents a technique for Nth-order differentiation of periodic pulse train. In addition to the interest in optical computing and information systems, Nth-order differentiators are of immediate interest for generation of Nth-order Hermite-Gaussian (HG) temporal waveform from an input Gaussian pulse, which can be used to synthesize any temporal shape by

#86081 - $15.00 USD Received 6 Aug 2007; revised 5 Sep 2007; accepted 6 Sep 2007; published 7 Sep 2007

superposition [1]. Several all-fiber schemes have been previously proposed based on long-period fiber gratings [2], phase-shifted fiber Bragg gratings (FBGs) [3,4], two-arm interferometer [5], and two oppositely chirped FBGs [6].

A schematic of the proposed general architecture is shown in Fig. 1. This approach exploits the well-known property of linearly-chirped FBGs, which apodization profile maps its spectral response [6-11]. The dispersion introduced by the FBG must meet two conditions: first, it must be high enough so the grating profile of the FBG maps the spectral response of the differentiator [8,9]. Second, it must meet the temporal Talbot condition [12], so dispersion does not affect to the waveform of the output pulses.

Besides the inherent advantages of FBGs (all-fiber approach, low insertion loss, and the potential for low cost), this scheme avoids the concatenation of N first order differentiator devices, which reduce energetic efficiency and increase the implementation complexity. Two different FBG based approaches have been previously demonstrated for all optical N-order time differentiation, namely multiple-phase-shifted FBG [4] and two oppositely chirped FBGs [6]. Concerning the first solution [4], it provides optical operation bandwidths in the tens-of-GHz, while our approach is specially suited for differentiating ultra-broadband optical waveforms (e.g. picosecond and sub-picosecond optical pulses). Regarding the second one [6], it requires two oppositely chirped FBGs, while this approach only requires one FBG. Furthermore, this approach can simultaneously multiply the input repetition rate. As a drawback, the system depends on the repetition rate of the input pulse train.

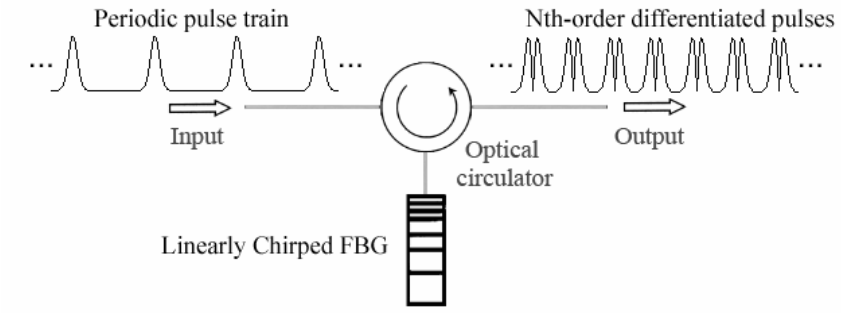

Fig. 1. Architecture of the system. Periodic pulse train is processed by an apodized linearly chirped FBG.

2. Theory

The analytic expression of an Nth-order differentiator in temporal domain is $f_{out}(t)=d^N f_{in}(t)/dt^N$, where $f_{in}(t)$ and $f_{out}(t)$ are the complex envelopes of the input and output of the system respectively, and t is the time variable. In frequency domain, $F_{out}(\omega)=(j\omega)^N F_{in}(\omega)$, where $F_{in}(\omega)$ and $F_{out}(\omega)$ are the spectral functions of $f_{in}(t)$ and $f_{out}(t)$, respectively (ω is the base-band frequency, i.e., $\omega=\omega_{opt}-\omega_0$, where ω_{opt} is the optical frequency, and ω_0 is the central optical frequency of the signals). Thus, an Nth-order differentiator is essentially a linear filtering device providing a spectral transfer function of the form $H_N(\omega)=F_{out}(\omega)/F_{in}(\omega)=(j\omega)^N$. We are interested in obtaining an analytic expression of a feasible spectral response, so the ideal spectral response function must be windowed, $H_{N,w}(\omega) = H_N(\omega)W(\omega) = (j\omega)^N W(\omega)$, where $W(\omega)$ is a window function.

The objective is to obtain a spectral response proportional to the differentiator spectral response. The chirped FBG introduces a dispersion term and we have $H_r(\omega)=\left(R(\omega)\right)^{1/2}\exp\left(j\phi_r(\omega)\right)\propto\left|H_{N,w}(\omega)\right|\exp\left(j\phi_N(\omega)+j\omega^2\ddot{\phi}_r/2\right)$, where $H_r(\omega)$, $R(\omega)$, and $\phi_r(\omega)$ are the spectral response in reflection, reflectivity and phase of the

#86081 - $15.00 USD Received 6 Aug 2007; revised 5 Sep 2007; accepted 6 Sep 2007; published 7 Sep 2007

FBG, $\phi_N(\omega)$=phase($H_N(\omega)$)=phase($H_{N,w}(\omega)$) and $\ddot{\phi}_r = \partial^2\phi_r(\omega)/\partial\omega^2$ is the first order dispersion coefficient of the FBG, which is a constant value for linearly chirped FBGs. Regarding the reflectivity, we have:

$$R(\omega) \propto \left|H_{N,w}(\omega)\right|^2 = \left|\omega^N W(\omega)\right|^2 \tag{1}$$

The refractive index of the FBG can be written as:

$$n(z) = n_{av}(z) + \frac{\Delta n_{\max}}{2} A(z)\cos\left[\frac{2\pi}{\Lambda_0} z + \varphi(z)\right] \tag{2}$$

where $n_{av}(z)$ represents the average refractive index of the propagation mode, Δn_{max} describes the maximum refractive index modulation, $A(z)$ is the normalized apodization function, Λ_0 is the fundamental period of the grating, $\varphi(z)$ describes the additional phase variation (chirp), and $z \in [-L/2, L/2]$ is the spatial coordinate over the grating, with L the length of FBG. In the following we consider a constant average refractive index $n_{av}=n_{eff}+(\Delta n_{max}/2)$, where n_{eff} is the effective refractive index of the propagation mode.

Notice that when N is odd, the differentiator spectral response presents a π-phase shift at ω=0. In our approach, this condition is attained by introducing a π-phase shift in the grating at z=0.

The chirp factor of the FBG, which is defined as $C_K=\partial^2\varphi(z)/\partial z^2$, and the length of the grating L, can be calculated from [13]:

$$C_K = -4n_{av}^2/(c^2\ddot{\phi}_r) \tag{3}$$

$$L = \left|\ddot{\phi}_r\right| c\Delta\omega_g \Big/ \left(2n_{av}\right) \tag{4}$$

where c is the light vacuum speed, and $\Delta\omega_g$ is the grating bandwidth.

The phase filtering of the FBG must be designed to cause a Talbot effect. In general, the pulses waveform of the periodic pulse train is affected by dispersion, but under Talbot condition [12] the pulses are reflected without undergoing distortion (self-image effect). This condition can be expressed as:

$$\left|\ddot{\phi}_r\right| = \frac{s}{m}\ \frac{T^2}{2\pi} \qquad \begin{matrix} s = 1,2,3,..., \\ m = 1,2,3,..., \end{matrix} \tag{5}$$

where s/m must be an irreducible rational fraction. Repetition rate multiplication can be achieved for m>1. As a result the reflected signal has a repetition rate m times that of the input signal.

Regarding the amplitude filtering, we apply an apodization profile to the grating that is accurately mapped on the spectral response under high dispersion condition [9], which can be expressed as:

$$\left|\ddot{\phi}_r\right| >> \left(\Delta t_g\right)^2 / 8\pi \tag{6}$$

#86081 - $15.00 USD Received 6 Aug 2007; revised 5 Sep 2007; accepted 6 Sep 2007; published 7 Sep 2007

where Δt_g can be calculated from the temporal length of $\Im^{-1}\left[H_{N,w}(\omega)\right]$, and $\Im^{-1}$ denotes inverse Fourier transform.

It is worth noting that in most cases $T^2 >> (\Delta t_g)^2$, and it is probable that (5) not only satisfies (6), but greatly exceeds it, so from (4) we can deduce that it is necessary to use a longer FBG than strictly required for space-to-frequency mapping.

The apodization profile can be obtained from the expression [8]:

$$A(z)=\left[-\ln\left(1-R(\omega)\Big|_{\left(\omega=sign(C_K)\frac{\Delta\omega_g}{L}z\right)}\right)\frac{32n_{av}^2}{\pi\omega_0^2\left|\ddot{\phi}_r\right|\Delta n_{\max}^2}\right]^{\frac{1}{2}} \tag{7}$$

3. Examples and results

In this section, examples of 1st and 4th order differentiators are designed and numerically simulated. We assume a carrier frequency ($\omega_0/2\pi$) of 193 THz, an effective refractive index n_{eff}=1.45, a band of interest ($\Delta\omega/2\pi$) of 5 THz centred at ω_0 (ω_0-$\Delta\omega/2 \le \omega_{opt} \le \omega_0$+$\Delta\omega/2$), a grating bandwidth $\Delta\omega_g=\Delta\omega$, a maximum reflectivity of 50 %, and a pulse train period T=40 ps.

For the first example (1st order differentiator) the corresponding ideal spectral response is $H_1(\omega)=j\omega$. We choose a function based on a hyperbolic tangent as window, $W(\omega)=W_{th}(\omega)=(1/2)[1+\tanh(4-|16\omega/\Delta\omega_g|)]$, and we have $H_{1,w}(\omega)=H_1(\omega)W_{th}(\omega)$. The desired reflectivity is obtained from (1):

$$R(\omega)=\left\{C_R\left(\omega/\Delta\omega_g\right)\left[1+\tanh\left(4-\left|16\omega/\Delta\omega_g\right|\right)\right]\right\}^2 \tag{8}$$

where C_R= 2.1238 is a normalization constant to get a maximum reflectivity of 50 %.

From the temporal length of $\Im^{-1}\left[H_{1,w}(\omega)\right]$ we obtain $\Delta t_g \approx 2$ ps. Using expressions (5) and (6) we have $\left|\ddot{\phi}_r\right|=\frac{s}{m}2.5464\times10^{-22}\ s^2/rad$ and $\left|\ddot{\phi}_r\right| >> 1.5915\times10^{-25} s^2/rad$. We choose $\ddot{\phi}_r=-1.2732\times10^{-22}\ s^2/rad$, where s=1 and m=2 have been selected. This implies that the input repetition rate is multiplied by two, so we have an output period of repetition $T_{out}= T_{in}/2$ =20 ps. The odd order of 1st differentiator implies that π-phase shift must be introduced in the grating at z=0.

Using (7), we obtain Δn_{max}=2.8160 × 10^{-4}, n_{av}=1.45014. Additionally, using (3) and (4), we obtain C_K=-7.3508×10^5 rad/m^2 and L=41.346 cm. The fundamental period of the grating can be obtained from $\Lambda_0=\pi c/(n_{av}\omega_0)$=535.574 nm. Finally, using (7) we obtain the apodization profile function:

$$A(z)=C_A\left(-\ln\left\{1-C_R^{\,2}\left|\frac{z}{L_a}\right|^{2N}\left[1+\tanh\left(4-\left|16\frac{z}{L_a}\right|\right)\right]^2\right\}\right)^{1/2} \tag{9}$$

where C_A=1.2011 is a normalization constant selected to get a normalized apodization profile function $0 \le A(z) \le 1$, and N=1.

#86081 - $15.00 USD Received 6 Aug 2007; revised 5 Sep 2007; accepted 6 Sep 2007; published 7 Sep 2007

As a second example we design a 4th-order differentiator using the same methodology. We obtain again $\Delta t_g \approx 2$ ps, and we design the same technological parameters as in the first example (so repetition rate is also doubled). The apodization profile is given by (9), where C_R=181.02, and N=4 (same L and C_A as for first example).

Figures 2(a), 2(b), and 2(c) show the results from our numerical simulations corresponding to the first example, and Fig. 2(d), 2(e), and 2(f) show the corresponding to second example. The spectral responses of the designed FBG and the ideal differentiator are showed in Fig. 2(a) and 2(d) for first and second example, respectively. The output pulse corresponding to an input gaussian pulse described by $f_{in,1}(t) \propto \exp(-t^2/(2\sigma^2))$ with σ= 800 fs, are showed in Fig. 2(b), and 2(e) for first and second example, respectively. The output pulse corresponding to an antisymmetric HG pulse described by $f_{in,2}(t) \propto \partial f_{in,1}(t)/\partial t \propto t \cdot \exp(-t^2/(2\sigma^2))$ are showed in Fig. 2(c), and 2(f) for first and second example, respectively.

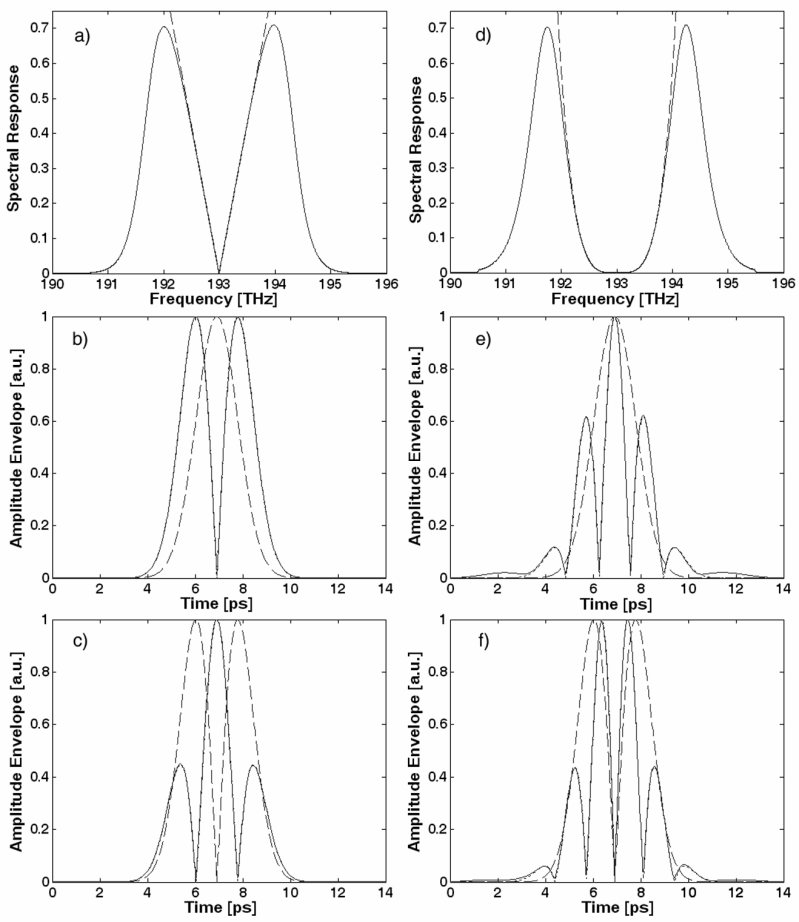

Fig. 2. Plots (a) and (d) show the amplitude of the spectral response corresponding to the FBG (solid), and to an ideal differentiator (dashed) for first and second examples, respectively. The temporal waveforms are showed in plots (b) and (c) for first example, and in plots (e) and (f) for second. Plots (b) and (e) correspond to a Gaussian pulse as input, and plots(c) and (f) correspond to an antisymmetric Hermite-Gaussian pulse as input. In plots (b), (c), (e) and (f) we show the input pulse in dashed line, the ouput pulse for the designed system in solid line, and the output pulse for the ideal differentiator in dotted line (indistinguishable from solid line in (b) and (c), and hardly distinguishable from solid line in (e) and (f)).

#86081 - $15.00 USD Received 6 Aug 2007; revised 5 Sep 2007; accepted 6 Sep 2007; published 7 Sep 2007

From (4) and (6) we obtain that the length of the grating requires $L >> 0.051$ cm for space-to-frequency, which can be satisfied from $L > 5$ cm. The length of the grating designed (41.346 cm) is much longer, but is within the accuracy of currently available fabrication techniques, as it can be seen in [11], where Talbot effect was achieved in a 96 cm linearly chirped FBG.

Considerations about the effect of group delay ripple can be found in [14], where it has been associated to the amplitude jitter of the rate-multiplied pulse train.

4. Conclusion

In this letter, an apodized linearly chirped FBG is designed and numerically simulated to simultaneously perform amplitude filtering to obtain the spectral response of the Nth-order differentiator, and phase filtering to cause temporal Talbot effect. The amplitude filtering exploits the fact that apodization profile of linearly chirped FBG maps its spectral response. This idea was used in a previous article published recently [6]. The main difference is that second chirped FBG for compensation of dispersion introducing by first FBG proposed in [6] is not required. This method reduces the number of required FBG to one and in addition the use of the Talbot effect allows repetition rate multiplication. These advantages must be weighed against the disadvantage that the system depends on the input repetition rate, and that the FBG length required for temporal Talbot effect can be much longer than the strictly required for space-to-frequency mapping.

It is worth noting that, unlike other pulse shaping techniques based on chirped FBGs [7-11], where the objective is shaping a specific output pulse from a known input pulse waveform, this system performs an operation (Nth-order temporal differentiation) than can be applied over different input waveforms to get the respective output waveforms.

Acknowledgements

This work was supported by the Spanish Ministerio de Educacion y Ciencia under Project "Plan Nacional de I+D+I TEC2004-04754-C03-02" and "Plan Nacional de I+D+I TEC2007-68065-C03-02".

#86081 - $15.00 USD Received 6 Aug 2007; revised 5 Sep 2007; accepted 6 Sep 2007; published 7 Sep 2007